Research Field: Outdoor environment
Research Year: FY2020
Research Number:20202013
Research Theme:Study on the impact of non-homogeneity of buildings on urban wind environment based on LES and wind tunnel experiments

Representative Researcher:Li Biao

Budget [FY2020]: 400,000Yen

*There is no limitation of the number of pages of this report.
*Figures can be included to the report and they can also be colored.
*Submitted reports will be uploaded to the JURC Homepage.

1. Research Aim

The main objective of this study is to evaluate the effect of horizontal and vertical heterogeneity on the flow characteristics and drag force distribution and thus to provide a foundation for improving the current parameterization of the urban canopy flow.

With this one year research work, we had three bullet points as below：

- Comparing and analyzing wind tunnel experiment and LES simulation results to reveal the influence mechanism of the heterogeneity of buildings on the ventilation characteristics and the pollutant dispersion in the non-uniform urban canopy;
- Jointly submit 1-2 high-level SCI academic papers and 1 conference presentation with JURC team.

The outcome of this study will provide experimental and theoretical support for aerodynamic parameters estimation on non-uniform buildings in the real urban area, increase the accuracy of the urban canopy models, and improve the precision of the urban weather forecast and the pollutant diffusion calculation.

2. Research Method

2.1 Large eddy simulation

The recycling method is used to generate inflow turbulent data for LES in a neutral boundary layer. Internal mapping, being one implementation of the recycling method, is adapted to this paper. The solution domain of the simulation is composed of two regions: (1) a driver region, where flow quantities are extracted from a cross section at a certain downstream location and recycled into the inlet, to generate the velocity fluctuations for the model region (2) a model region for simulating flow over the target model.

The simulation is initialized with turbulent 3-dimensional velocities which are mapped from a precursor simulation with cyclic boundaries and same topography as the driver region of the solution domain. Besides, the constant volume is conserved and the wind profile from the wind tunnel experiments initializes the precursor simulation.

The instantaneous wind velocities of the simulation at the inflow of the driver region are calculated as follows,

$$u_{inlet} = U_z + \varphi \times [u - U_{av}]_{rec} \tag{1}$$

$$v_{inlet} = \varphi \times [v - V_{av}]_{rec} \tag{2}$$

$$w_{inlet} = \varphi \times [w - W_{av}]_{rec} \tag{3}$$

$$\varphi = 0.5 \left\{ 1 - \frac{\tanh\left[\frac{8.0(\theta - 1.0)}{4.0(0.3 - \theta) + 0.7}\right]}{\tanh(8.0)} \right\} \tag{4}$$

where U_z is stream-wise velocity which is averaged horizontally and temporally from the simulation results of the precursor run. U_{av}, V_{av}, W_{av} are temporally averaged stream-wise velocities. u, v, w are instantaneous velocity components. The subscript 'inlet' and 'rec' denote the variables at the inlet and the recycling planes. $\theta=z/\delta$, δ is the boundary layer thickness. φ is the damping factor.

The *PALM* (**PA**rallelized **L**ES **M**odel), open source code developed by Leibniz University Hannover is used in this paper. It is especially designed for performing on massively parallel computer architectures, and so far have tested up to 32,000 cores. *PALM* has been widely used in many research fields, such as the turbulent airflow in street canyon, the turbulent structure of urban boundary layer, urban wind environment and pollutant dispersion. *PALM* adopts LES turbulence model, in which eddies smaller than cut-off length is modelled while large eddies are directly resolved. The filtered Navier-Stokes equations are as follows:

$$\frac{\partial \overline{u}_i}{\partial x_i} = 0 \tag{5}$$

$$\frac{\partial \overline{u}_i}{\partial t} + \overline{u}_j \frac{\partial \overline{u}_i}{\partial x_j} = -\frac{1}{\rho}\frac{\partial \overline{p}}{\partial x_j} - \frac{\partial}{\partial x_j}\left(\upsilon \frac{\partial \overline{u}_i}{\partial x_j}\right) - \frac{\partial \tau_{ij}}{\partial x_j} \tag{6}$$

where u_i and u_j are the velocity components, ρ and υ are density and viscosity. The overbar symbol denotes the filtering operator, and τ_{ij} is the subgrid scale stress (SGS) term defined as:

$$\tau_{ij} = \overline{u_i u_j} - \overline{u}_i \overline{u}_j \tag{7}$$

The Boussinesq hypothesis is used to calculate the SGS stress term, and a modified version of Deardorff's subgrid-scale model is adopted as follows,

$$\tau_{ij} - \frac{2}{3} e \delta_{ij} = -\upsilon_{SGS}\left(\frac{\partial \overline{u}_i}{\partial x_j} + \frac{\partial \overline{u}_j}{\partial x_i}\right) \tag{8}$$

$$\upsilon_{SGS} = C_m l e^{\frac{1}{2}} \tag{9}$$

where ν_{SGS} is the SGS turbulent viscosity; e is the SGS turbulent kinetic energy (TKE); C_m of 0.1 is the model constant, l is the SGS mixing length. For neutral boundary layer, it depends on the

altitude from the wall z, grid spacing, and is calculated as follows:

$$l = \min\left(1.8z, (\Delta x \Delta y \Delta z)^{\frac{1}{3}}\right) \tag{10}$$

Moreover, the model closure includes a prognostic equation for the SGS-TKE e, under neutral boundary layer, is calculated as follows,

$$\frac{\partial e}{\partial t} = -\overline{u_j}\frac{\partial e}{\partial x_j} - \tau_{ij}\left(\frac{\partial u_i}{\partial x_j}\right) + \frac{\partial}{\partial x_j}\left(2\upsilon_{SGS}\frac{\partial e}{\partial x_i}\right) - \epsilon) \tag{11}$$

where ϵ is the dissipation rate within a grid volume,

$$\epsilon = C_\epsilon \frac{e^{\frac{1}{2}}}{l} \tag{12}$$

The coefficient C_ϵ is specified as 0.93. To reduce the impact of the outflow on the inner flow state, all the variables normal to the outflow boundary are set as zero gradient. Periodic boundary condition is used for the span-wise of the computational domain, and free slip condition is used as the top boundary condition. Wall functions are based on Monin-Obukhov similarity theory, so the sub-grid stress of the first vertical layer τ_{i3} is calculated as below：

$$\tau_{i3} = -\left[\frac{\overline{u_r}}{log(z_s/z_0)}\right]^2 \frac{\overline{u_i}}{\overline{u_r}} \tag{13}$$

where, z_0 is roughness length, κ is Von Karman constant, being set as 0.4; z_s is the altitude at the first vertical grid; z_0 is set 0.0005 m (0.1 m in full scale); $u_r = (u^2 + v^2)^{1/2}$ is the resolved resultant horizontal velocity at the first vertical grid.

The advection term of *N-S* equation adapts the 5th order upwind scheme of Wicker and Skamarock. The time step scheme used for the integration of the prognostic variables is 3th order Runge-Kutta scheme. Calculation grid and discrete operation are used as implicit filter to the N-S equation, and the turbulence field is divided into resolved scale and sub-grid scale. The Poisson solvers for pressure use multigrid method. The physical time step Δt is dynamically adjusted to meet the criterion that *CFL* number is no more than unity. The simulation time is 40 s. For the first 10 s, the flow reaches a quasi-steady state. Sliding average of 10 s data among the rest of 30 s for mean velocity and turbulence intensity profiles behave insignificant changes, therefore 10 s is used to perform time-averaging for LES results. The simulations were performed with 36 cores Intel Xeon Gold 2.30 GHz CPUs with 256 GB RAM.

The atmospheric boundary layer wind tunnel experiments were performed in the small section of the Wind Tunnel and Wave Trough Laboratory of Harbin Institute of Technology. The experimental design diagram is shown in Fig. 1. Following the load code for the design of building structures of China (*GB 50009-2012*), the turbulent inflow arrangement adopts the standard *C*-type terrain, which represents the approaching flow over the dense areas such as trees, gentle hilly land, low-rise buildings and high-rise buildings. The terrain roughness index in power-law profile is 0.22. The fetch length is 19.2 m, and the thickness of the boundary layer is about 1.3 m. The tested building array is shown schematically in Fig. 2, with geometric scale of 1/200. The building array

consists of total 23 cuboids with uniform size of 213.7mm (length) × 144.4mm (width) × 105mm (height). The plane area density is 27.5%, and frontal area density is 25%. The blockage ratio is 1.9%. For concise, the $B_{i,j}$ is used to represent building model, where i represents the row number coordinate, and j represents the column number coordinate. The pressure taps were arranged on the six white blocks $B_{i,3}$ along the wind direction in Fig. 2.

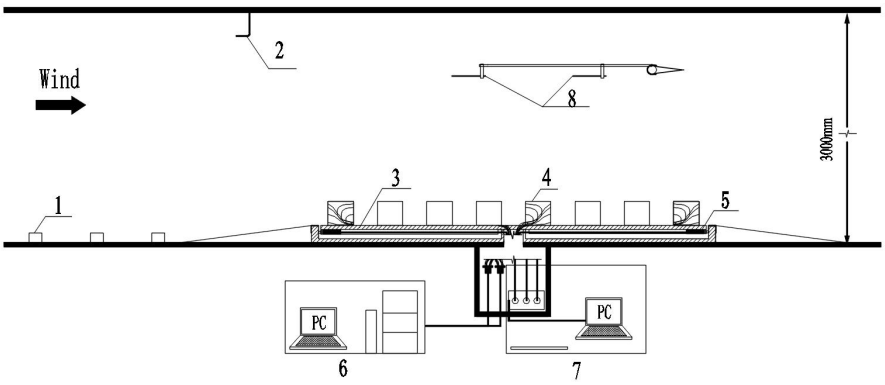

Fig. 1 Schematic diagram of wind tunnel platform. 1Terrain roughness elements, 2 Pitot-static tube, 3 Floating device, 4 Pressure module, 5 Force sensor, 6 Pressure scanning valve system, 7 Force sensor system. 8 Hot-wire anemometers.

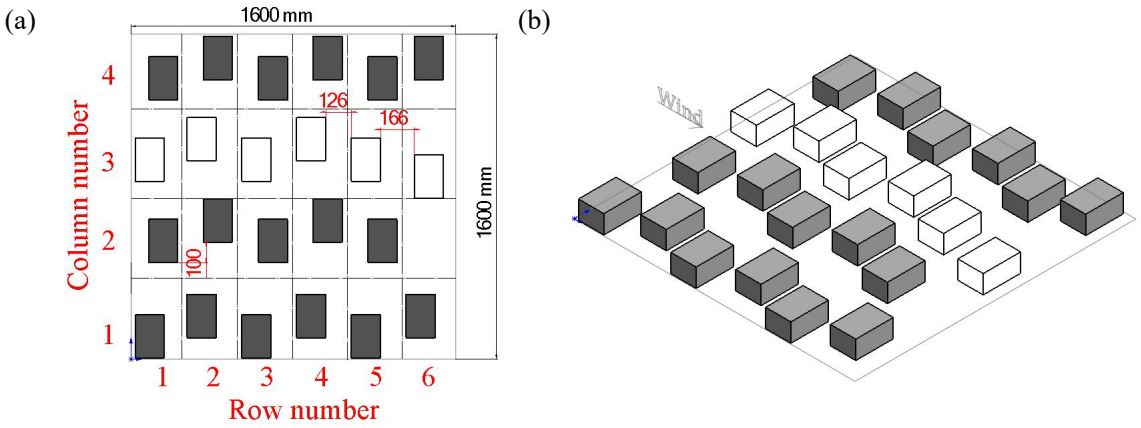

Fig. 2 Schematic diagrams of block arrangements. (a) Plan view (b) Isometric view. The white blocks are used for pressure measurement. The array comprises 6 rows × 4 columns, with the absence of one building model at the sixth row and second column, total 23 blocks.

2.2 Wind tunnel experiment

The atmospheric boundary layer wind tunnel experiment was carried out in a low-speed test section of the wind tunnel of Wind Engineering Research Center of Shijiazhuang Tiedao University. The rectangular section of the experimental section is 4.4 m wide and 3 m high, and the length of small experimental section is 24 m. The maximum wind velocities that the wind tunnel are capable of producing are greater than 30.0 m/s.

The schematic diagram of wind tunnel platform is shown in Fig. 3. The planar area of the base

board is 1.6 × 1.6 m^2. Measurements of the current test mainly consisted of the surface pressure, the reference velocity, and the velocity profile of the incoming flow.

(a)

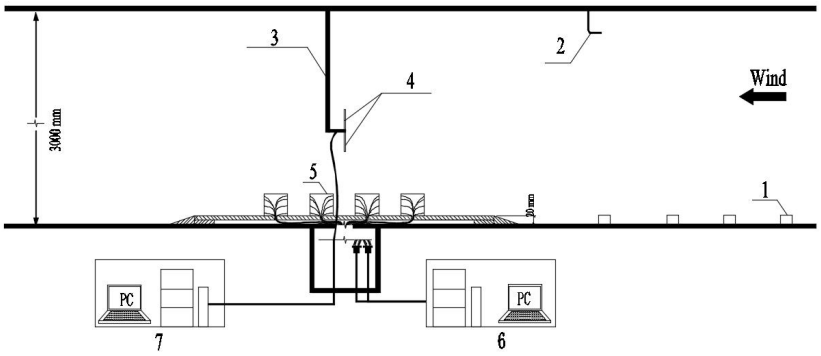

(b)

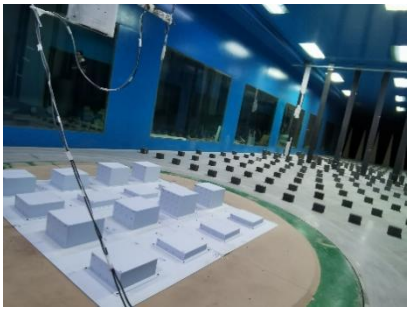

(c)

Fig. 3 (a) Schematics of the wind tunnel platform. 1Terrain roughness elements, 2 Pitot-static tube, 3 Auto vertical mask for Cobra probe, 4 Three-component velocity Cobra probe, 5 Pressure modules, 6 Pressure scanning valve system, 7 Measurement system for three-component velocity Cobra probe. (b) Inside views of the wind tunnel with H2 andR1casesasrepresentatives (c) Two Cobra probes, which are named as *A* and *B* respectively.

The testing building array is shown schematically in Table 1, with a geometric scale of 1/150. The building arrays consist of two layouts: staggered and aligned layouts. Meanwhile each layer was subtracted separately and considered as the case condition.

The rough surfaces used for the measurement were regular arrays of sharp-edged blocks, and glued onto thin plastic plates. All blocks had a uniform base of 200 mm ×200 mm; hereafter, L = 200 mm is the basic length scale. The details of the arrays summarized in Table1.

Table 1 Test conditions

	Aligned layout		Staggered layout	
Property	Arrays	Configuration	Arrays	Configuration
Separate layer conditions	AL1	Layer 1，H=40 mm	-	-
	AL2	Layer 2，H=40 mm	ST2	Layer 2，H=40 mm
	AL3	Layer 3，H=40 mm	ST3	Layer 3，H=40 mm
	AL4	Layer 4，H=40 mm	ST4	Layer 4，H=40 mm
	AL5	Layer 5，H=180 mm	-	-

Multiple layer conditions	AL12	Layer 1 + Layer 2	ST12	Layer 1 + Layer 2
	AL13	Layer 1 + Layer 2 + Layer 3	ST13	Layer 1 + Layer 2 + Layer 3
	AL14	Layer 1 + Layer 2 + Layer 3+ Layer 4	ST14	Layer 1 + Layer 2 + Layer 3+ Layer 4
	AL15	Layer 1 + Layer 2 + Layer 3 + Layer 4+ Layer 5	ST15	Layer 1 + Layer 2 + Layer 3+ Layer 4 + Layer 5
Contrast condition	AL0	H=106 mm	-	-

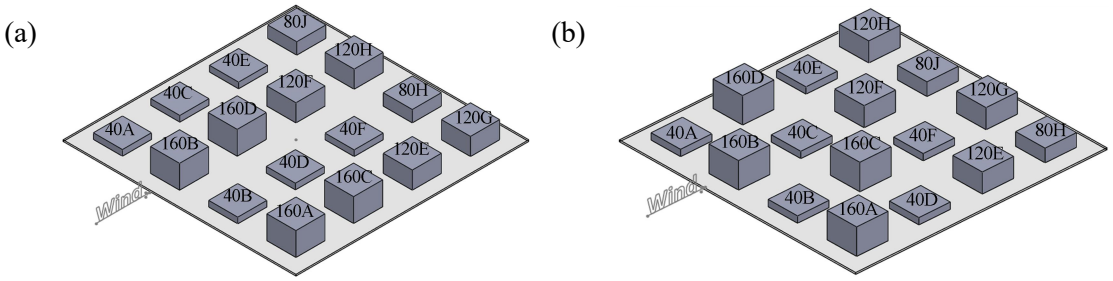

Fig. 4 The experimental diagram for (a) case AL14 and (b) case ST14

3. Research Result

3.1 Large eddy simulation

The turbulent characteristics are examined without and with the immersed buildings. The average values of the four points of the 400 mm×400 mm square in the center of the model area are taken as the spatial average. Flow characteristics obtained from LES and experiment without the immersing building array are shown in Fig. 5. It can be concluded that the mean wind velocity as well as the turbulence intensity of stream-wise velocity component I_u are consistent with the experimental results.

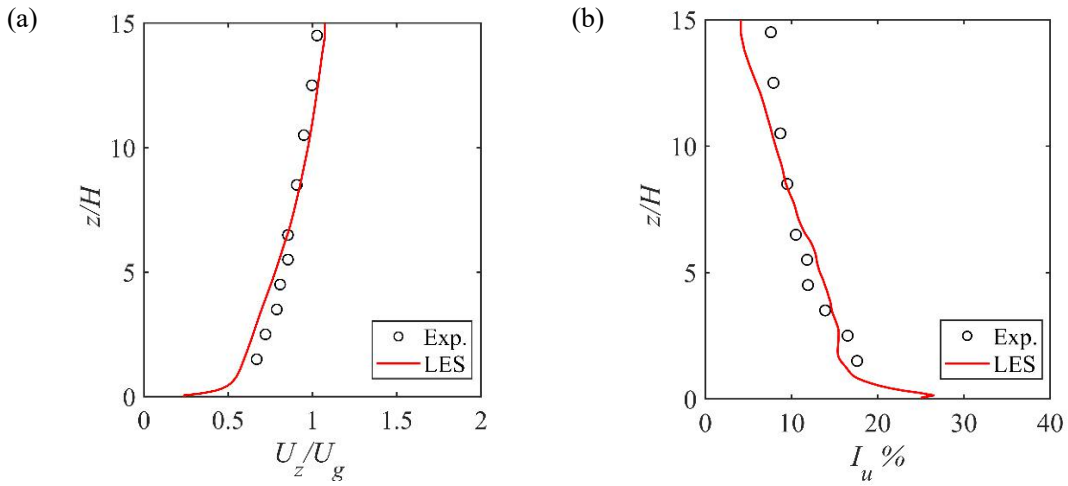

Fig. 5. Approaching flow characteristics obtained from LES and experiment without immersing building models. (a) Normalized stream-wise mean velocity U_z/U_g, where U_g is the mean wind velocity at boundary layer height δ. (b) Stream-wise turbulence intensity I_u.

To investigate the flow characteristics for the flow over horizontal non-uniform buildings, Q-criterion is adapted, shown in Fig. 6. We can see that the instantaneous vortex structures present distinct randomness and fragmentation. For the first row of buildings, the horseshoe-type vortex at the windward face can be clearly observed. In addition, the incoming flow clearly separates at the roof of the first row of buildings, therefore creating strong shear stress. The columnar vortexes formed by the shear layer are transported downstream, resulting in a higher velocity near the roof than in other areas.

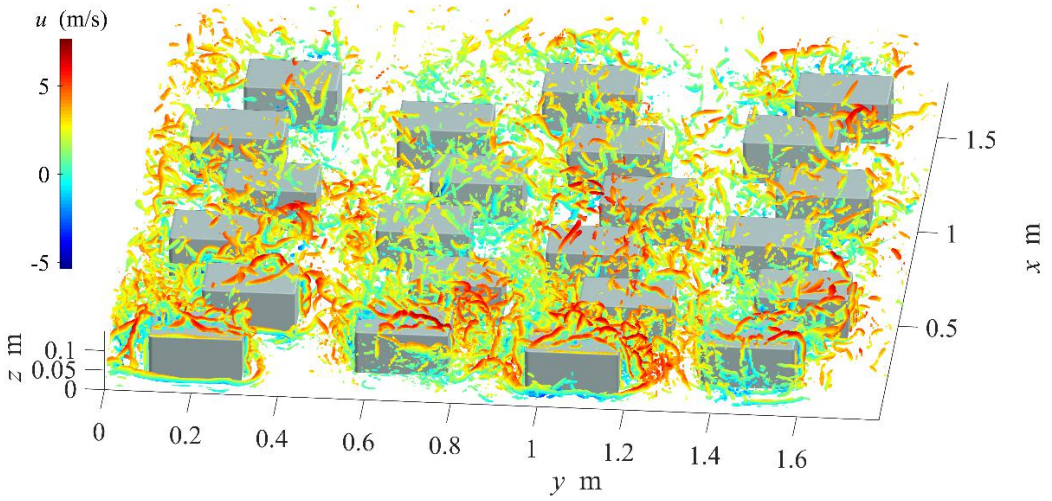

Fig 6. Instantaneous iso-surface of Q criterion, where Q equals to 3×10^4. The color chart shows magnitude of instantaneous velocity.

(a)

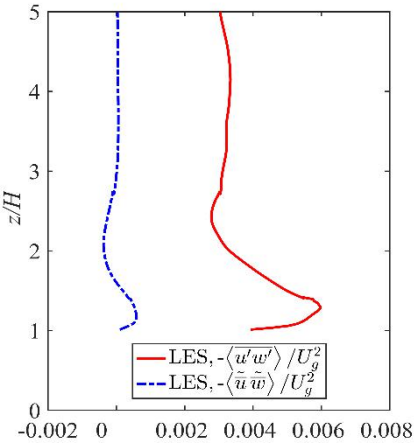

(b)

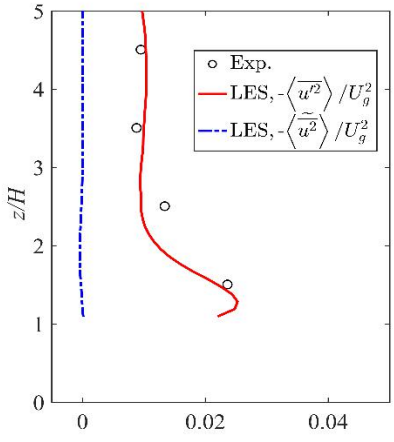

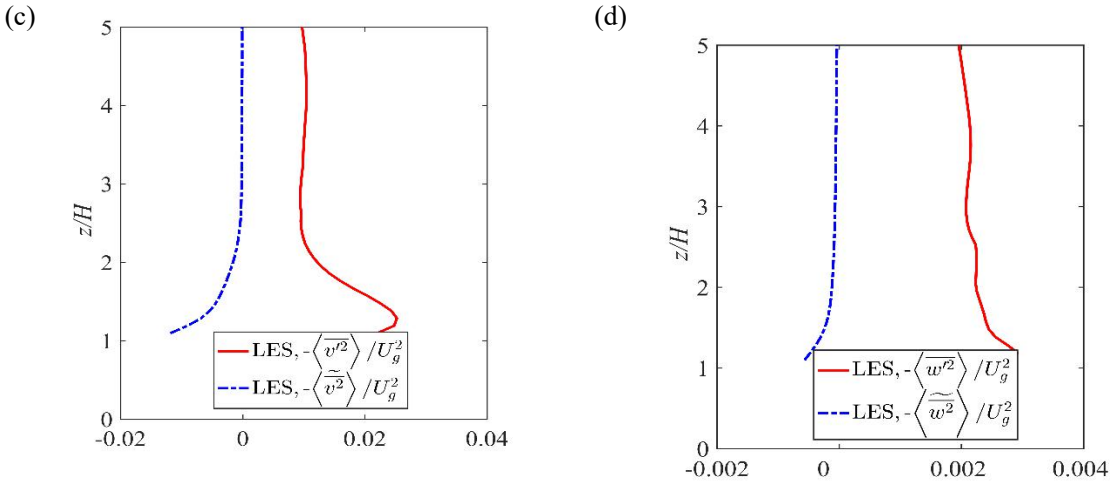

Fig. 7 The dispersive stress components $-\langle\widetilde{U}\widetilde{W}\rangle$, $-\langle\widetilde{U}^2\rangle$, $-\langle\widetilde{V}^2\rangle$ $-\langle\widetilde{W}^2\rangle$, Reynolds stress components $-\langle\overline{u'w'}\rangle$, $-\langle\overline{u'^2}\rangle$, $-\langle\overline{v'^2}\rangle$, $-\langle\overline{w'^2}\rangle$ above the canopy layer, normalized by U_g^2,

Fig. 7 displays the profiles of normalized spatial averaged Reynolds stresses and dispersive stresses. Above the canopy layer, total shear stress is mainly contributed by Reynolds stress, $-\langle\overline{u'w'}\rangle$, and for the dispersive stress $\langle\widetilde{u}\widetilde{w}\rangle$, is zero when z/$H$ is larger than 3, which means a roughness sublayer exists within this height, and dispersive stress plays a role in the roughness sublayer as well. These results are also common for other dispersive stress and Reynolds stress components. This is due to the non-uniformity of building array characterized by the existence of ventilation corridors, yielding the spatial inhomogeneity of the mean velocity and dispersive stress above the canopy layer.

3.2 Wind tunnel experiment

Following the load code for the design of building structures of China (*GB 50009-2012*), the wind tunnel arranges the standard C-type terrain (Load code for the design of building structures, GB 50009-2012, in China), which represents the dense areas such as trees and low-rise buildings, high-rise buildings, gentle hilly land. The terrain roughness index (in power-law profile) is 0.22. In current experiment, the fetch length is 19.2 m, and the thickness of the boundary layer δ is around 1.5 m, estimated by taking the height at which the velocity is 99% of the reference velocity. Fig. 8 shows the profiles of incoming velocity and turbulent intensities.

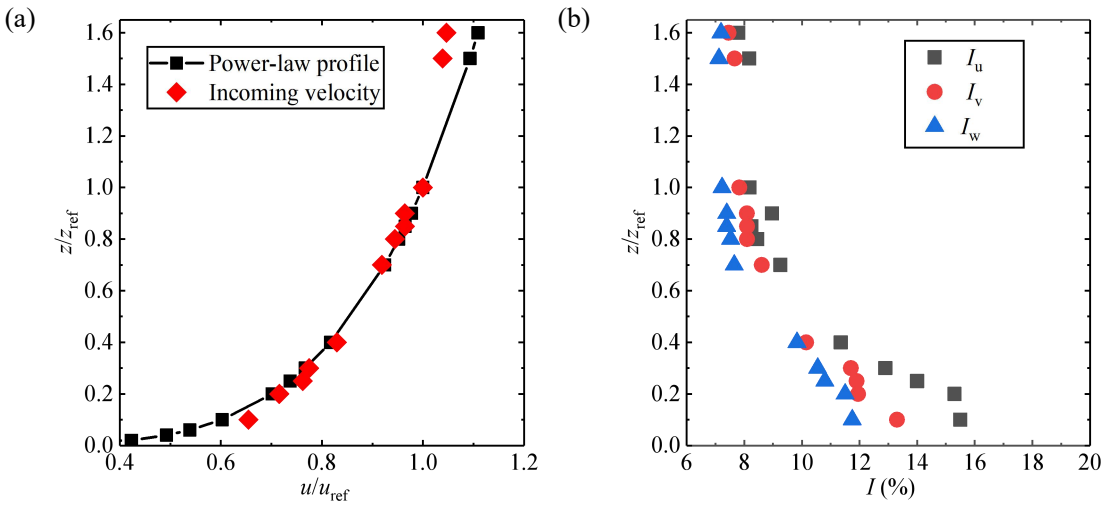

Fig. 8. Approaching flow characteristics without immersing building models. (a) Stream-wise mean velocity u/u_{ref}, where u_{ref} is the mean wind velocity at boundary layer height δ. (b) turbulence intensities I_u, I_v, and I_w.

Besides, δ is adapted to represent the relative error of drag force after stacking of single-story buildings, and it is calculated as following:

$$\delta = \frac{\Delta p(i)_{S4} - \Delta p(1)_{Li}}{\Delta p(1)_{Li}} \times 100\% \tag{14}$$

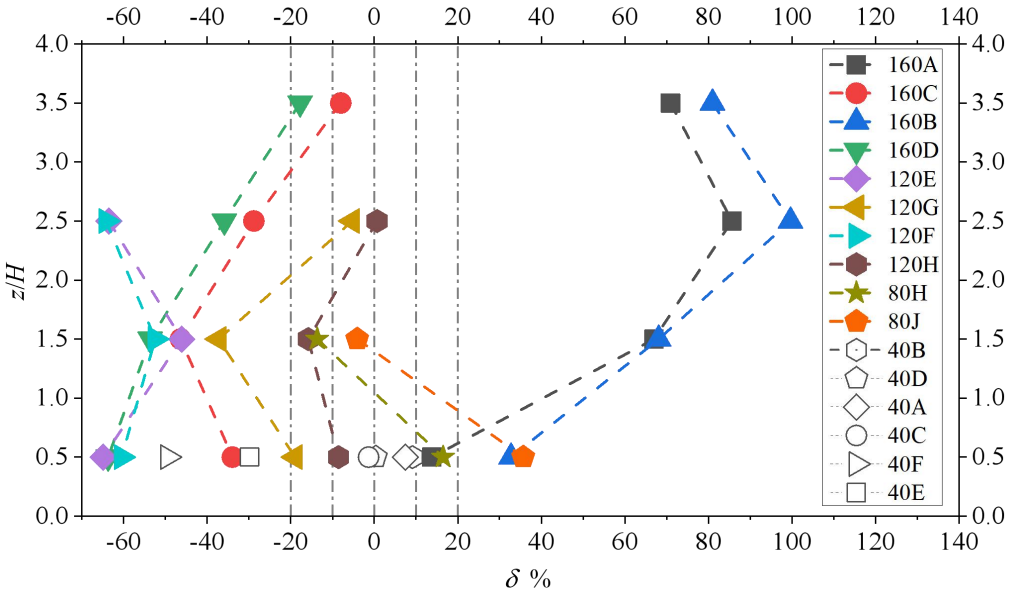

Fig. 9. The relative error of drag force after stacking of single-story buildings for aligned layout.

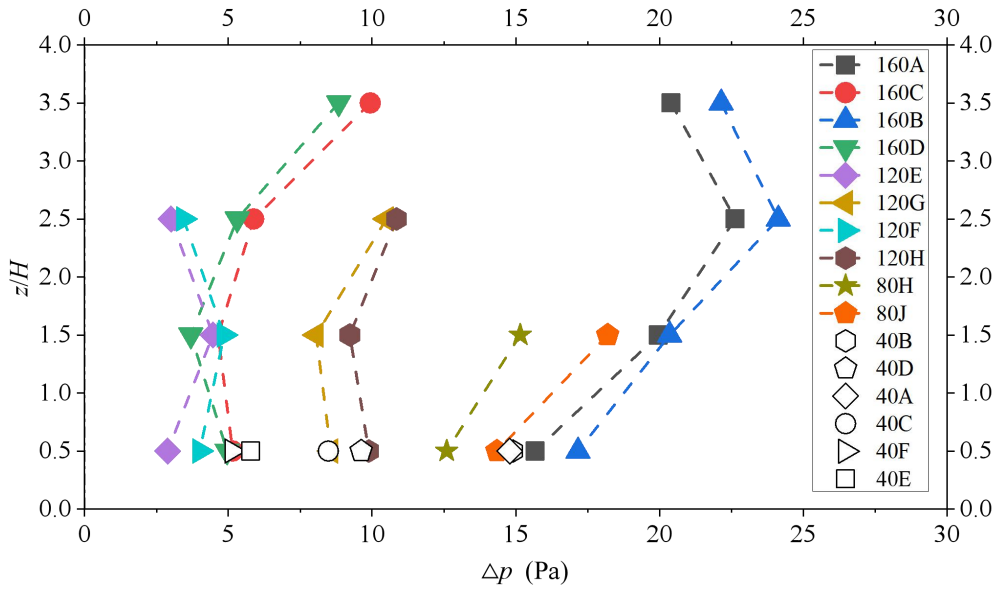

Fig. 10. The pressure difference △p for all building models for aligned layout.

From Fig. 9-10, it can be concluded that the main drag is provided by windward buildings 40A, 40B, 160A, 160B and 80J, 80H in the first row of windward buildings. For i =2(that is, z/H=1.5), for 80J,80H, i =3, for 120G,120H, i =4, for 160D,160C, δ is within (-20% 20%), indicating that the building superimposed along the negative direction of height has little influence on the single-storey building. For i =3, 120F,120E, i =4, for 160B and 160A, δ is larger, because 160B and 160A are windward buildings, and there are taller buildings in front of 120E and 120F, leading to the change of air flow pattern. For buildings 120E and 120F, the building is superimposed along the positive and negative directions in the wake area of the high-rise building in front, which has a great influence on the drag characteristics of the upper and lower buildings. For 120G and 120H buildings, located in the flow recovery zone, the buildings are superimposed along the positive and negative directions, which have a great influence on the building of this layer, and less influence on the drag characteristics of the upper and lower buildings. For buildings 80H and 80J, the superstructure is superimposed along the positive direction, which has a great influence on the building on the floor and a little influence on the drag characteristics of its superstructure. For 40C, 40D, 40E, and 40F, the change in height of the surrounding buildings has less effect on the drag characteristics of the building because its location is in the inner part of the building complex and the change in flow pattern is more moderate. For windward buildings 160B,160A, the impact of stacking buildings on this floor is greater in various ways.

4. Published Paper etc.
[Underline the representative researcher and collaborate researchers]
[Published papers]
1. WANG Lu, LIU Jing, JIANG Cunyan, LI Biao*, SONG Di, LU Ming, XUAN Yinli, Large eddy simulation of drag distributions of flow over non-uniform building arrays, Sustanible City and Society, submitted.

[Presentations at academic societies]
1. Study on the parameterization and aerodynamic effects of non-uniform buildings, Research Seminar on Urban Heat & Wind Environments (Online)，2021.3.4, JURC, Japan
2.

[Published books]
1.
2.

[Other]
Intellectual property rights, Homepage etc.

5. Research Group
1. Representative Researcher
LI Biao
2. Collaborate Researchers
1. WANG Lu
2. JIANG Cunyan
3. LIU Jing
4. XUAN Yingli

6. Abstract (half page)

Research Theme:

Study on the impact of non-homogeneity of buildings on urban wind environment based on LES and wind tunnel experiments

Representative Researcher (Affiliation)

LI Biao*, WANG Lu, LIU Jing, JIANG Cunyan (Harbin Institute of Technology)

XUAN Yinli (Tokyo Polytechnic Unversity)

This study evaluates the effect of horizontal and vertical heterogeneity on the flow characteristics and drag force distribution and thus to provide a foundation for improving the current parameterization of the urban canopy flow. Large-eddy simulation (LES) based on the modified Smagorinsky model was employed to simulate the flow and drag characteristics of a non-uniform building array. An inflow turbulence generation technique based on Kataoka's method was utilized with the initial conditions generated by the roughness elements in the recycling region. Numerical simulation of a wind tunnel experiment setup is conducted with and without the building arrays. The method was validated by comparing with experimental data. We also conduct a new wind tunnel experiment to explore the effect of height variation on the drag force. Results revealed that given appropriate arrangements of roughness elements and initial conditions, the calculated mean flow variables and their fluctuations agreed well with the experimental data. The mean and unsteady flow fields around the building arrays are discussed, to explore the corresponding drag distributions. The outcome of this study will provide experimental and theoretical support for aerodynamic parameters estimation on non-uniform buildings in the real urban area, increase the accuracy of the urban canopy models, and improve the precision of the urban weather forecast and the pollutant diffusion calculation.